

CHAPTER 3

A GENERALIZED ELECTROCHEMICAL MODEL FOR HIGH- κ DIELECTRIC AND NANOMATERIAL BASED ENFETS

CHAPTER 3

A generalized electrochemical model for high- κ dielectric and nanomaterial based ENFETs

3.1. High- κ dielectric and nanomaterial based ENFETs

The high- κ dielectric and nanomaterial based ENFETs consists of high- κ dielectric materials such as HfO_2 , ZrO_2 , Ta_2O_5 , etc. as the gate insulating material and nanomaterials such as graphene and CNT as the substrate. Graphene and CNT forms good interface with high- κ dielectrics as discussed in Chapter 2. Few graphene and CNT based ENFETs with high- κ dielectrics, as insulating material has been fabricated displaying excellent characteristics and response [6-8]. To study the behavior of such devices, a model is desired. In order to develop a generalized electrochemical model for such ENFET devices, the basic structure of the device needs to be known. Considering the fabricated nanomaterial based ENFET devices, the general structure of such ENFETs along the diffusion length (x) with the enzyme-insulator interface as origin has been shown in Fig. 3.1. The structure consists of a bottom substrate on which the whole device is fabricated. On top of the substrate, an insulating material is present which prevents leakage of current from the nanomaterial towards the bottom substrate. The high- κ dielectric is present on the nanomaterial. Enzyme sensing layer is deposited on the high- κ dielectric material to hold the enzymes. Enzymes directly cannot be immobilized on the dielectric, so, enzyme sensing layer is required which extends from origin (0) to length of enzyme sensing membrane (L_e). The device is immersed in the electrolyte solution, which consists of the biomolecules to be detected.

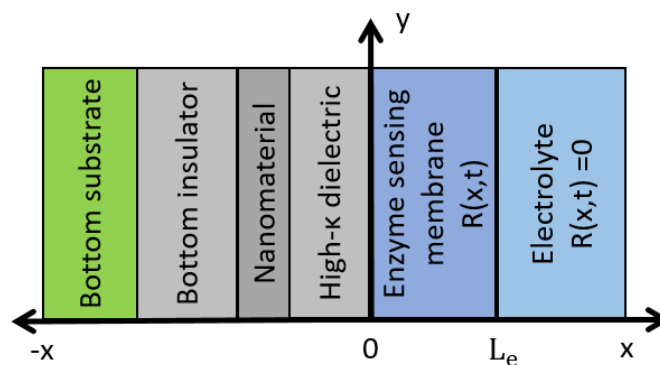


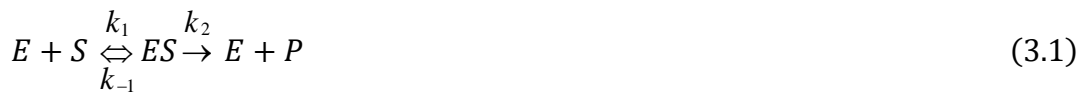
Fig. 3.1. General structure of high- κ dielectric nanomaterial based ENFET device

3.2. ENFET modeling

As discussed in the previous section, the whole ENFET device can be divided into different layers. The variations that occur in one layer is transferred to the other layer from electrolyte towards the nanomaterial. Firstly, the enzymes act upon the biomolecules to give the products. The substrate and product diffuses into the enzyme sensing layer following the Fick's law of diffusion. The products produces pH variations at the oxide surface, which results in potential variation at the surface. The variation in surface potential varies the threshold voltage of the device, which is the input parameter for the ENFET. These variations in threshold voltage at different concentration of the biomolecules produces different drain current values, which can be measured. Thus, modeling of ENFET device is done in different phases. The key steps involved in the unique approach for electrochemical modeling of ENFETs are discussed in details in the later sub-sections.

3.2.1. Modeling of enzymatic reactions

The rate of enzymatic reactions depends on the concentration of the biomolecules involved in the reaction. The relation between concentration of biomolecules and the rate of enzymatic reactions is established using the Michaelis Menten equation. The relationship is found out using an enzymatic reaction as given below [34]:



where, E, S, P and ES represents enzyme, substrate, product and enzyme substrate intermediate respectively. k_1 and k_2 are the rate of forward reaction resulting in formation of enzyme substrate intermediate and product respectively and k_{-1} is the rate of backward reaction resulting in formation of substrate. Therefore, the rate of formation of enzyme substrate intermediate should be equal to its breakdown

$$k_1[E][S] = k_{-1}[ES] + k_2[ES] \quad (3.2)$$

$$[ES] = \frac{k_1[E][S]}{k_{-1} + k_2} = \frac{[E][S]}{K_M} \quad (3.3)$$

$$\text{where, } K_M = \frac{k_{-1} + k_2}{k_1} \quad (3.4)$$

The total enzyme concentration, E_0 , is given as,

$$[E_0] = [E] + [ES] \quad (3.5)$$

$$[ES] = \frac{([E_0] - [ES])[S]}{K_M} = \frac{[E_0][S]}{[S] + K_M} \quad (3.6)$$

The rate of formation of products is given by

$$\frac{dP}{dT} = a = k_2[ES] = k_2 \frac{[E_0][S]}{[S] + K_M} \quad (3.7)$$

$$a = a_M \frac{[S]}{[S] + K_M} \quad (3.8)$$

This equation is known as Michaelis Menten equation and $a_M = k_2[E_0]$, is the maximal enzyme activity for one enzyme unit. K_M is known as Michaelis Menten constant, which is the substrate concentration at which the reaction rate is half of a_M .

3.2.2. Modeling of the diffusion phenomena of substrate and products in electrolyte

The substrate biomolecules present in the electrolyte solution diffuses into the enzymatic layer, where the enzymatic reactions occur giving products. The diffusion of substrate and product biomolecules follows the Fick's law of diffusion. If $[S]$ denotes the substrate concentration and $[P]$ denotes the product concentration, then following the Fick's second law of diffusion, the variations in $[S]$ and $[P]$ can be modeled as shown in Eqs. (3.9) and (3.10) respectively [16].

$$\frac{\partial[S](x, t)}{\partial t} = D_S \frac{\partial^2[S](x, t)}{\partial x^2} - R(x, t) \quad (3.9)$$

$$\frac{\partial [P](x, t)}{\partial t} = D_P \frac{\partial^2 [P](x, t)}{\partial x^2} + R(x, t) \quad (3.10)$$

where, D_S and D_P are the diffusion coefficients of substrate and product present in the electrolyte solution.

The diffusion constant is calculated using the Archimede's law and Einstein's equation. As per Archimede's law, the equivalent volumic mass ρ' of a spherical molecule having equivalent radius r' and mass m when diluted in a given fluid of volumic mass ρ and viscosity η is similar to the fluid volumic mass ρ . Hence, according to the Einstein's equation, the fluidic diffusion coefficient D of the studied molecules can be found as shown by Eq. (3.11) [15]:

$$D = \frac{kT}{6\pi\eta r'} = \frac{1}{6\pi\eta} \sqrt[3]{\frac{4\pi\rho' N_{AV}}{3M}} kT = \frac{1}{6\pi\eta} \sqrt[3]{\frac{4\pi\rho N_{AV}}{3M}} kT = A_f \frac{kT}{\sqrt[3]{M}} \quad (3.11)$$

where, k is the Boltzmann constant, M is the molar mass of the molecule under study, T is the absolute temperature, N_{AV} is the Avogadro's number and A_f is a fluid dependent constant.

R represents the enzymatic reactions in the enzymatic layer (length L_e) as shown in Fig. 3.1. The origin for measurement of length is taken at the enzyme insulator interface. The length L_e , of the enzyme layer which is also called enzyme layer thickness is measured from the origin. As seen in Eq. (3.12), all the enzymatic activities occur in the region from 0 to L_e . Beyond which, the activities are negligible and considered to be almost zero. So, all the calculations are done in this region.

$$\left. \begin{aligned} R(x, t) &= a_M n_{enz} \frac{[S](x, t)}{[S](x, t) + K_M}, & 0 \leq x \leq L_e \\ R(x, t) &= 0, & x > L_e \end{aligned} \right\} \quad (3.12)$$

where, n_{enz} is the number of enzymatic units per volume unit in the enzyme sensing layer.

For solving the Eqs. (3.9) and (3.10), to obtain $[S]$ and $[P]$, certain initial and boundary conditions are required which can be set as per enzyme kinetics. Accordingly, initially

(i.e. at $t = 0$) when no reaction takes place, $[S]$ and $[P]$ are zero in the region from 0 to L_e . The boundary conditions are defined at $x = 0$ (i.e. interface of oxide and enzyme layer) and $x = L_e$ (i.e. interface of enzyme layer and bulk electrolyte). As per enzyme kinetics, the substrate biomolecules diffuse from bulk electrolyte to the enzyme layer, but products formed in the enzyme layer do not diffuse back into the electrolyte. Instead, they bind with the sites available at the oxide-enzyme interface in accordance with the site binding theory. Therefore, the variations in substrate and product concentrations is negligible with respect to x at $x = 0$. Again, at $x = L_e$, the substrate concentration is taken to be equal to the initial substrate concentration as the enzymatic reactions are almost negligible here and hence, the product concentration is zero. In the bulk electrolyte beyond the enzyme layer, almost no reactions take place, therefore, no variation occur in substrate and product concentrations here. Thus, the initial and boundary conditions are shown in Eq. (3.13).

$$\begin{array}{l}
 \text{at } t = 0, 0 \leq x \leq L_e: [S](x, t) = 0, [P](x, t) = 0 \\
 \text{at } t > 0, x = 0: \frac{\partial[S](x, t)}{\partial x} = 0, \frac{\partial[P](x, t)}{\partial x} = 0 \\
 \text{at } t > 0, x = L_e: [S](x, t) = S_0, [P](x, t) = 0 \\
 \text{at } x > L_e: [S](x, t) = S_0, [P](x, t) = 0
 \end{array} \quad (3.13)$$

Now, considering steady state response, the time derivative will be set to zero, so, Eqs. (3.9) and (3.10) reduces to the form,

$$\frac{\partial^2[S](x, t)}{\partial x^2} = \frac{R(x, t)}{D_S} \quad (3.14)$$

$$\frac{\partial^2[P](x, t)}{\partial x^2} = - \frac{R(x, t)}{D_P} \quad (3.15)$$

Using the boundary conditions, the Eqs. (3.14) and (3.15) are solved to get the substrate and product concentrations. The solutions can be done either numerically without any limiting condition or analytically using three limiting cases either $[S] \ll K_M$ or $[S] \gg K_M$ or $[S] \approx K_M$ as shown under.

Case 1: $[S] \ll K_M$

This case represents enzyme kinetics that is much faster than the transport through the enzymatic layer, the substrate concentration being the limiting factor. Applying this condition, Eq. (3.12) reduces to the form as given below

$$\left. \begin{aligned} R(x, t) &= a_M n_{enz} \frac{[S](x, t)}{K_M}, & 0 \leq x \leq L_e \\ R(x, t) &= 0, & x > L_e \end{aligned} \right\} \quad (3.16)$$

Using Eq. (3.16) in Eq. (3.14) we get,

$$\begin{aligned} D_S \frac{\partial^2 [S](x, t)}{\partial x^2} &= a_M n_{enz} \frac{[S](x, t)}{K_M}, & 0 \leq x \leq L_e \\ \Rightarrow \frac{\partial^2 [S](x, t)}{\partial x^2} - \alpha [S](x, t) &= 0, & 0 \leq x \leq L_e \end{aligned} \quad (3.17)$$

where, $\alpha = \frac{a_M n_{enz}}{D_S K_M} = \frac{k_2 [E_0]}{D_S K_M}$ = enzyme loading factor/diffusion modulus.

Integrating Eq. (3.17) and using the boundary conditions for substrate concentration from Eq. (3.13) we get,

$$\begin{aligned} \int_{x=0}^{L_e} \frac{\partial^2 [S](x, t)}{\partial x^2} &= \alpha \int_{x=0}^{L_e} [S](x, t), & 0 \leq x \leq L_e \\ [S](x, t) &= \frac{\cosh(x\sqrt{\alpha})}{\cosh(L\sqrt{\alpha})} [S](L_e, t), & 0 \leq x \leq L_e \end{aligned} \quad (3.18)$$

Putting $[S](L_e, t)$ in Eq. (3.14), we get,

$$\frac{\partial [S](L_e, t)}{\partial t} = -a_M n_{enz} \frac{[S](L_e, t)}{K_M}, \quad \left[\because D_S \frac{\partial^2 [S](x, t)}{\partial x^2} = 0 \right]$$

Integrating the above equation, we get,

$$\ln([S](L_e, t)) = -\frac{a_M n_{enz} t}{K_M} + C$$

At $t = 0$, $[S](L_e, t) = S_0 \Rightarrow C = \ln(S_0)$

$$\begin{aligned} \therefore \ln([S](L_e, t)) &= -\frac{a_M n_{enz} t}{K_M} + \ln(S_0) \Rightarrow \ln\left(\frac{[S](L_e, t)}{S_0}\right) = -\frac{a_M n_{enz} t}{K_M} \\ \Rightarrow [S](L_e, t) &= \exp\left(-\frac{a_M n_{enz} t}{K_M}\right) S_0 \end{aligned} \quad (3.19)$$

The product concentration can be determined from the substrate concentration. From Eqs. (3.14) and (3.15) we get,

$$D_S \frac{\partial^2 [S](x, t)}{\partial x^2} + D_P \frac{\partial^2 [P](x, t)}{\partial x^2} = 0 \quad (3.20)$$

In the above equation, the kinetic term $R(x, t)$ is removed. Integrating the above equation for $0 \leq x \leq L_e$, we get,

$$\begin{aligned} D_S \int_{x=0}^{L_e} \frac{\partial^2 [S](x, t)}{\partial x^2} + D_P \int_{x=0}^{L_e} \frac{\partial^2 [P](x, t)}{\partial x^2} &= C \\ \Rightarrow D_S \frac{\partial [S](x, t)}{\partial x} + D_P \frac{\partial [P](x, t)}{\partial x} &= C \end{aligned} \quad (3.21)$$

At the insulating surface, $x = 0$, the product concentration $[P]_{x=0} = [P]_0$ is desired as it is proportional to the output signal of the ENFET.

Integrating Eq. (3.21), we get,

$$\begin{aligned} D_S [S](L_e, t) + D_P [P](L_e, t) &= D_S [S](x, t) + D_P [P](x, t) = C, \quad 0 \leq x \leq L_e \\ \Rightarrow D_P [P](x, t) &= D_S [S](L_e, t) + D_P [P](L_e, t) - D_S [S](x, t) \\ &= D_S [S](L_e, t) - D_S \frac{\cosh(x\sqrt{\alpha})}{\cosh(L_e\sqrt{\alpha})} [S](L_e, t) + D_P [P](L_e, t) \\ \Rightarrow [P](x, t) &= \frac{D_S}{D_P} \left[1 - \frac{\cosh(x\sqrt{\alpha})}{\cosh(L_e\sqrt{\alpha})} \right] [S](L_e, t) + [P](L_e, t) \end{aligned} \quad (3.22)$$

$$\text{At } x = 0, [P]_0 = \frac{D_S}{D_P} \left[1 - \frac{1}{\cosh(L_e\sqrt{\alpha})} \right] [S](L_e, t) + [P](L_e, t)$$

Putting $[P](L_e, t)$ in Eq. (3.10), we get,

$$\frac{\partial [P](L_e, t)}{\partial t} = a_M n_{enz} \frac{[S](L_e, t)}{K_M} \Rightarrow [P](L_e, t) = - \exp\left(-\frac{a_M n_{enz} t}{K_M}\right) S_0 + C$$

$$\text{At } t = 0, [P](L_e, t) = 0 \therefore C = S_0$$

$$\therefore [P](L_e, t) = S_0 - \exp\left(-\frac{a_M n_{enz} t}{K_M}\right) S_0 \quad (3.23)$$

Case 2: $[S] \gg K_M$

This case represents very high substrate concentration that saturates the enzyme. Applying this condition, Eq. (3.12) reduces to the form as given below

$$\left. \begin{aligned} R(x, t) &= a_M n_{enz} \quad , \quad 0 \leq x \leq L_e \\ R(x, t) &= 0 \quad , \quad x > L_e \end{aligned} \right\} \quad (3.24)$$

Using Eq. (3.24) in Eq. (3.14), we get,

$$D_S \frac{\partial^2 [S](x, t)}{\partial x^2} = a_M n_{enz} \Rightarrow \frac{\partial^2 [S](x, t)}{\partial x^2} = \frac{a_M n_{enz}}{D_S} \quad , \quad 0 \leq x \leq L_e$$

Integrating the above equation for $0 \leq x \leq L_e$, we get,

$$\Rightarrow \int_{x=0}^{L_e} \frac{\partial^2 [S](x, t)}{\partial x^2} = \int_{x=0}^{L_e} \frac{a_M n_{enz}}{D_S}$$

$$\frac{\partial [S](x, t)}{\partial x} = \frac{a_M n_{enz}}{D_S} x + C = \alpha' x + C, \quad 0 \leq x \leq L_e \quad (3.25)$$

$$\text{where, } \alpha' = \frac{a_M n_{enz}}{D_S}$$

Using the first boundary condition for substrate concentration in Eq. (3.25), we get,
 $C = 0$

Again, integrating Eq. (3.25), we get,

$$\int_{x=0}^{L_e} \frac{\partial[S](x, t)}{\partial x} = \int_{x=0}^{L_e} \alpha' x \Rightarrow [S](x, t) = \frac{\alpha' x^2}{2} + C_1, \quad 0 \leq x \leq L_e$$

Using the second boundary condition, we get,

$$C_1 = [S](L_e, t) - \frac{\alpha' L_e^2}{2}$$

$$\therefore [S](x, t) = [S](L_e, t) + \frac{\alpha'}{2}(x^2 - L_e^2)$$

$$\Rightarrow [S](x, t) = [S](L_e, t) + \frac{a_M n_{enz}}{2D_S}(x^2 - L_e^2), \quad 0 \leq x \leq L_e \quad (3.26)$$

Putting $[S](L_e, t)$ in Eq. (3.9), we get,

$$\frac{\partial[S](L_e, t)}{\partial t} = -a_M n_{enz}$$

Integrating the above equation we get,

$$[S](L_e, t) = -a_M n_{enz} t + C$$

At $t = 0$, $[S](L_e, t) = S_0$, $\therefore C = S_0$

$$\therefore [S](L_e, t) = -a_M n_{enz} t + S_0 \quad (3.27)$$

Again,

$$D_P[P](x, t) = D_S[S](L_e, t) + D_P[P](L_e, t) - D_S[S](x, t), \quad 0 \leq x \leq L_e$$

$$\Rightarrow D_P[P](x, t) = D_S[S](L_e, t) + D_P[P](L_e, t) - D_S \left\{ [S](L_e, t) + \frac{a_M n_{enz}}{2D_S}(x^2 - L_e^2) \right\}$$

$$\Rightarrow [P](x, t) = [P](L_e, t) - \frac{a_M n_{enz}}{2D_P}(x^2 - L_e^2) \quad (3.28)$$

Placing $[P](L_e, t)$ in Eq. (3.10), we get,

$$\frac{\partial[P](L_e, t)}{\partial t} = a_M n_{enz} \Rightarrow [P](L_e, t) = a_M n_{enz} t + C$$

At $t = 0$, $[P](L_e, t) = 0$, $\therefore C = 0$

$$\therefore [P](L_e, t) = a_M n_{enz} t \quad (3.29)$$

Case 3: $[S] \approx K_M$

In this case, the substrate concentration is comparable to enzyme kinetics. Applying this condition, Eq. (3.12) reduces to the form as given below

$$\left. \begin{aligned} R(x, t) &= \frac{a_M n_{enz}}{2}, & 0 \leq x \leq L_e \\ R(x, t) &= 0, & x > L_e \end{aligned} \right\} \quad (3.30)$$

Solving Eqs. (3.9) and (3.10) as per the above condition we get,

$$[S](x, t) = [S](L_e, t) + \frac{a_M n_{enz}}{4D_S} (x^2 - L_e^2) \quad (3.31)$$

$$[P](x, t) = [P](L_e, t) - \frac{a_M n_{enz}}{4D_P} (x^2 - L_e^2) \quad (3.32)$$

where,

$$[S](L_e, t) = -\frac{a_M n_{enz} t}{2} + S_0 \quad (3.33)$$

$$[P](L_e, t) = \frac{a_M n_{enz} t}{2} \quad (3.34)$$

Now, for the condition $x > L_e$, i.e. going beyond the enzyme layer, deep into the bulk electrolyte, the substrate and product concentrations are determined as shown below.

As $R(x, t) = 0$, so, Eq. (3.9) becomes,

$$\frac{\partial [S](x, t)}{\partial t} = D_S \frac{\partial^2 [S](x, t)}{\partial x^2}$$

Assuming steady state, we get, $\frac{\partial^2 [S](x, t)}{\partial x^2} = 0$

Integrating, we get, $\frac{\partial [S](x, t)}{\partial x} = C = 0$ $\left[\because \frac{\partial [S](x, t)}{\partial x} = 0 \text{ at } x = \infty \right]$

Integrating the above equation, we get,

$$[S](x, t) = C = S_0 \quad [\because [S](x, t) = S_0 \text{ at } x = \infty]$$

$$\therefore [S](x, t) = S_0, \quad x > L_e \quad (3.35)$$

$$\text{Again, } \frac{\partial [P](x, t)}{\partial t} = D_p \frac{\partial^2 [P](x, t)}{\partial x^2}$$

$$\text{Assuming steady state, we get, } \frac{\partial^2 [P](x, t)}{\partial x^2} = 0$$

$$\text{Integrating, we get, } \frac{\partial [P](x, t)}{\partial x} = C = 0 \quad \left[\because \frac{\partial [P](x, t)}{\partial x} = 0 \text{ at } x = \infty \right]$$

Integrating the above equation, we get,

$$[P](x, t) = C = 0 \quad [\because [P](x, t) = 0 \text{ at } x = \infty]$$

$$\therefore [P](x, t) = 0, \quad x > L_e \quad (3.36)$$

In this way, the concentration of products is obtained which further contributes to acid/base reactions resulting in pH variations at the oxide surface.

3.2.3. Modeling of acid/base reactions of the product in the electrolyte

The product produced in the reactions releases H^+/OH^- ions depending on whether it is acidic or basic. The resulting concentration of H^+ ions can be determined by solving the equations obtained by using various parameters such as acid dissociation constant of the product (K_a), water ionic product (K_w), charge neutrality concept and the acid/basic properties of the initial solution (C_i).

Let us consider $[HA]$ to be the product involved in production of H^+ ions as given in Eq. (3.37). Therefore, the acid dissociation constant is given by Eq. (3.38).



$$K_a = \frac{[A^-][H^+]}{[HA]} \quad (3.38)$$

Water can be both an acid and a base. This results in the equilibrium reaction given by Eq. (3.39). This equilibrium reaction gives water ionic product as given by Eq. (3.40).



$$K_e = [H^+][OH^-] \quad (3.40)$$

The initial value of acid/basic nature of the solution can be determined by using the pH of the buffer solution (pH_0) and the water ionic product as shown in Eq. (3.41) [16]. The charge neutrality concept is shown in shown in Eq. (3.42).

$$C_i = 10^{-pH_0} - 10^{-(pK_e - pH_0)} \quad (3.41)$$

$$[H^+] = [A^-] + [OH^-] + C_i \quad (3.42)$$

Solving the Eqs. (3.38) to (3.42), the we get the concentration of H^+ ions. These equations and solutions may vary depending on the nature of product. The resulting pH of the solution is determined based on the concentration of H^+ ions produced as given by Eq. (3.43).

$$pH(x, t) = -\log[H^+](x, t) \quad (3.43)$$

The values of pH , thus obtained at different diffusion length is further used to determine the surface potential at the oxide-electrolyte interface.

3.2.4. ISFET Modeling

The modeling of ISFET corresponds to the surface potential variation at the oxide-electrolyte interface due to pH variations. This can be done by using the Bousse's model, which has been discussed in details in Chapter 2. In this model, leaving aside the pH variations, the other factors that affect are the sensitivity parameter β and the point of zero charge pH_{pzc} . These factors depend on K_a and K_b , which are the equilibrium constants at the acid and base point respectively. The equilibrium constants are almost fixed for a particular dielectric under certain conditions. Use of different dielectric materials in a device as gate insulator varies the device sensitivity.

The sensitivity s of the device can be obtained from the Bousse model equation as shown in Eq. (3.44). It is the measure of the surface potential with the change in pH of the electrolyte at the surface of the insulator. It depends on the factor β , which shifts the sensitivity from the Nernstian sensitivity of 59 mV/pH. Since, the β value is different for different insulating material, the sensitivity of the device also varies. Greater the value of β , the factor $\beta/(\beta + 1)$ approaches closer to unity and the device sensitivity approaches closer to Nernstian sensitivity.

$$S = \frac{\psi}{\Delta pH} = 2.303 \frac{kT}{q} \frac{\beta}{\beta + 1} \quad (3.44)$$

To test the sensitivity variation, different dielectric materials i.e. SiO₂, Al₂O₃, HfO₂, ZrO₂, Ta₂O₅ and TiO₂ were used and the simulation was done using MATLAB tool. The pH of the electrolyte was varied from 2-12 and consequently the other measurements were taken. The known values of dissociation constants and other calculated parameters for Al₂O₃, HfO₂, ZrO₂, Ta₂O₅ and TiO₂ are listed in Table 3.1 at 25 °C. The pH_{pzc} value is found to be different for different dielectric materials. The site density from the available literature is taken. Taking C_{eq} as 20 μFcm^{-2} and N_S values from Table 3.1, the β value was calculated for different dielectrics followed by the sensitivity. Fig. 3.2 shows the surface potential variation with pH for different dielectric materials depicting variations in sensitivity. It is seen that Al₂O₃ has a very low sensitivity as compared to the other materials, whose sensitivity are almost comparable. The sensitivity has been found highest for Ta₂O₅ and ZrO₂, which is comparable to Nernstian sensitivity. Thus, the use of high- κ dielectric material is preferred over low- κ materials.

3.2.5. Current transport model for high- κ dielectric nanomaterial based ENFETs

The change in potential seen in the previous section affects the threshold voltage and hence, the drain current of the device. In nanomaterial based FET such as G-ENFET and CNT-ENFET, the Si substrate is replaced by graphene and CNT respectively. From the fabricated device characteristics of such ENFETs [6-8], it was observed that nanomaterial based ENFETs behave like MOSFET. Moreover, from structural point of view ENFETs closely resemble MOSFET, so, the MOSFET or ISFET current

equations can be used along with the threshold voltage of ENFET as the input parameter ($V_{TH,ENFET}$).

Table 3.1. Sensitivity of different dielectrics at 25 °C

Gate Insulating Material	Dielectric Constant (κ)	pK_a	pK_b	pH_{pzc}	Site Density N_S (cm^{-2})	β	Sensitivity S (mV/pH)
Al_2O_3	9	10	6	8 [100]	8×10^{14}	4.98	49.3
ZrO_2	25	7	5	6 [75]	10×10^{14}	62.2	58.2
HfO_2	25	9	6	7.5 [72]	10×10^{14}	19.68	56.3
Ta_2O_5	26	4	2	3 [100]	10×10^{14}	62.25	58.3
TiO_2	80	7.4	4.94	6.17 [19]	10×10^{14}	36.65	57.6

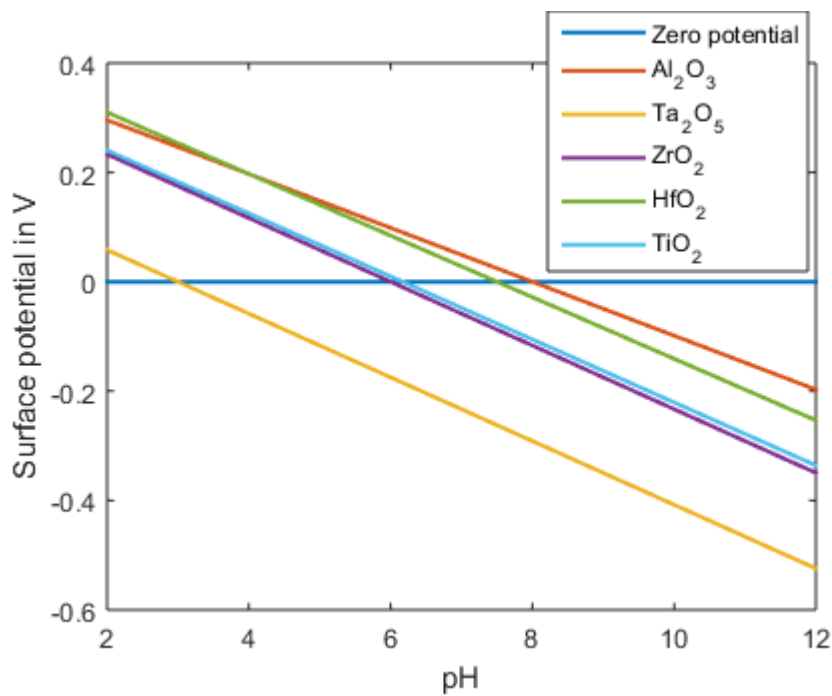


Fig. 3.2. Surface potential variation with pH for different dielectric materials depicting variations in sensitivity

The current equations for ENFET in linear and saturation regions are given by Eqs. (3.45) and (3.46) respectively.

$$I_{DS,lin} = \mu \frac{W}{L} V_{DS} C_{ox} \{ (V_{GS} - V_{TH,ENFET}) - 0.5 V_{DS} \} \quad (3.45)$$

$$I_{DS,sat} = \mu \frac{W}{2L} C_{ox} (V_{GS} - V_{TH,ENFET})^2 \quad (3.46)$$

The determination of threshold voltage of nanomaterial based ENFETs is the critical factor. The calculation of parameters involved in the threshold voltage equation is different for graphene and CNT based ENFETs. It has been discussed in the later chapters. A sample code of the developed model in MATLAB tool has been shown in Appendix A.

3.3. Summary

In this chapter, the generalized steps required to develop an electrochemical model for high- κ dielectric nanomaterial based ENFETs has been shown. It is seen that the modeling is done in different phases considering the variations in the device layer by layer. From the modeling steps it can be summarized that the main activities on which ENFET modeling depends are the enzymatic reactions on the substrate biomolecules, diffusion phenomena of the main substrate in the electrolyte, acidic or basic reactions of the product in the electrolyte, the pH detection properties of ISFET and the current transport model of the nanomaterial based ENFET. The difference arises in the threshold voltage determination for different nanomaterials used as substrate. Moreover, for different biomolecules the acid/base reactions leading to the pH variations may vary. From the developed generalized model, it was found that the most influential parameters which produce variations in the device performance are K_M , n_{enz} , $[S]$, K_a , pH_{pzc} , pH_0 , β , N_s , $V_{TH,ENFET}$, κ , μ , W , L and C_{ox} . Based on these parameters, the validation of the generalized model has been carried out using three different nanomaterial based ENFET devices as shown in the succeeding chapters.